# Ultrasound Deep Brain Stimulation Regulates Food Intake and Body Weight in Mice

Wen Meng, Zhengrong Lin, Tianyuan Bian, Xiaoyan Chen, *Student Member, IEEE*, Long Meng, *Member, IEEE*, Tifei Yuan, Lili Niu, and Hairong Zheng, *Senior Member, IEEE*

***Abstract*— Given the widespread occurrence of obesity, new strategies are urgently needed to prevent, halt and reverse this condition. We proposed a noninvasive neurostimulation tool, ultrasound deep brain stimulation (UDBS), which can specifically modulate the hypothalamus and effectively regulate food intake and body weight in mice. Fifteen-min UDBS of hypothalamus decreased 41.4% food intake within 2 hours. Prolonged 1-hour UDBS significantly decreased daily food intake lasting 4 days. UDBS also effectively restrained body weight gain in leptin-receptor knockout mice (Sham: 96.19%, UDBS: 58.61%). High-fat diet (HFD) mice treated with 4-week UDBS (15 min / 2 days) reduced 28.70% of the body weight compared to the Sham group. Meanwhile, UDBS significantly modulated glucose-lipid metabolism and decreased the body fat. The potential mechanism is that ultrasound actives pro-opiomelanocortin (POMC) neurons in the hypothalamus for reduction of food intake and body weight. These results provide a noninvasive tool for controlling food intake, enabling systematic treatment of obesity.**

***Index Terms*— Transcranial ultrasound, acoustic radiation force, neuromodulation, food intake, obesity.**

## I. Introduction

OBESITY is an increasingly prevalent health issue worldwide with significant economic repercussions [1], [2], [3]. In particular, it is strongly associated not only with increasing chances of suffering from diabetes, coronary heart disease, certain cancer, depression, and anxiety [1], but also with premature mortality at all ages [4], [5]. Hence, obesity cannot be treated as a cosmetic issue bothering some individuals, but rather as a threatening pandemic to global health. Hypothalamus is considered a major nucleus regulating appetite [6], [7]. Physical (electrical, optical) stimulation of the hypothalamus for appetite control has attracted extensive attention in recent years [8], [9]. Deep brain stimulation (DBS) of the hypothalamus can regulate energy balance and treat obesity [10], and optogenetics can regulate appetite and significantly decrease food intake in rodents [8], [11], [12], proving the value of physical neuromodulation methods in appetite management and obesity treatment. However, DBS and optogenetics are inherently invasive and require brain implants. Consequently, new technology is needed to noninvasively stimulate the hypothalamus to control food intake and body weight.

Transcranial ultrasound offers a non-invasive way to focalize energy to deep brain regions [13], [14], [15]. Rodent, nonhuman primate and human studies have experimentally proven that low-intensity ultrasound can produce effective neuromodulation without evidence of neurologic injury [13], [14], [15], [16], [17], [18], [19], [20], [21]. Ultrasound stimulation can significantly decrease ischemic lesions in ischemic stroke rat models [22], [23], [24] and reduce recovery time in mice with traumatic brain injury [25]. In addition, ultrasound stimulation of epileptic foci has been shown to inhibit seizure activity [26], [27], [28], [29], [30]. Recent studies by our research group have demonstrated that ultrasound deep brain stimulation (UDBS) of the motor cortex or deep brain region (subthalamic nucleus or globus pallidus) can improve motor function in mouse models of Parkinson's disease [17], [31], [32], [33]. Ultrasound neuromodulation targeting primary somatosensory cortex can regulate evoked cortical activity and enhance somatosensory discrimination of humans [13], while targeting cortical areas in patients with Alzheimer's disease can induce neuropsychological improvements and upregulation of memory networks [34]. Stimulation of the thalamus in patients with disorder of consciousness altered thalamic connectivity which correlates with subsequent behavioral recovery [35]. However, it remains uncertain whether ultrasound stimulation of hypothalamus can control the food intake and body weight.

Manuscript received 22 May 2023; revised 4 August 2023, 8 October 2023, and 25 December 2023; accepted 2 January 2024. Date of publication 9 January 2024; date of current version 19 January 2024. This work was supported in part by the National Natural Science Foundation of China under Grant T2122023 and Grant 12022410, in part by the Youth Innovation Promotion Association of the Chinese Academy of Sciences (CAS) under Grant 2020358, in part by the Guangdong Basic and Applied Basic Research under Grant 2021B1515120045, and in part by the Shenzhen Basic Science Research under Grant JCYJ20220818101608018. *(Wen Meng and Zhengrong Lin contributed equally to this work.) (Corresponding authors: Lili Niu; Hairong Zheng.)*

Wen Meng, Zhengrong Lin, and Xiaoyan Chen are with the Shenzhen Institutes of Advanced Technology, Chinese Academy of Sciences, Shenzhen 518055, China, and also with the Shenzhen College of Advanced Technology, University of Chinese Academy of Sciences, Shenzhen 518055, China.

Tianyuan Bian, Long Meng, Lili Niu, and Hairong Zheng are with the Shenzhen Institutes of Advanced Technology, Chinese Academy of Sciences, Shenzhen 518055, China (e-mail: ll.niu@siat.ac.cn; hr.zheng@siat.ac.cn).

Tifei Yuan is with the Shanghai Key Laboratory of Psychotic Disorders, Shanghai Mental Health Center, Shanghai Jiao Tong University School of Medicine, Shanghai 200030, China.

Digital Object Identifier 10.1109/TNSRE.2024.3351312

In this study, a wearable transducer (frequency: 3.8 MHz, 2 g weight) and the suitable collimators with different apertures were designed and fabricated for freely moving mice. The relevance of the aperture diameter to the focusing situation was evaluated by simulation and measurement. We achieved large depth ultrasound stimulation of the hypothalamus, especially of the arcuate nucleus (ARC) with a subcranial depth of about 6 mm. We also identified an acoustic parameter set that selectively increases activity of pro-opiomelanocortin (POMC) neurons in the hypothalamus. These selective parameters achieved significant food intake and body weight suppression in three mouse models, providing an innovative tool for non-invasive intervention and treatment of overweight or obesity.

## II. Materials and Methods

### A. Animal Preparation

Male C57BL/6J mice (8 weeks, Beijing Vital River Laboratory Animal Technology Co. Ltd), BKS-Leprem2Cd479/Gpt mice (6 weeks, Nanjing GemPharmatech Co., Ltd.), POMC-CreER::Ai14 mice and NPY-CreER::Ai14 mice (7-9 weeks) were used for the experiments. All animal experiments were done following the guidelines approved by the Institutional Ethical Committee of Animal Experimentation of the Shenzhen Institutes of Advanced Technology, Chinese Academy of Sciences and the Laboratory Animal Guidelines of Welfare and Ethics. The IACUC number was SIAT-IACUC-210308-YGS-NLL-A1745. Animals were maintained in an environment with constant temperature ($23 \pm 1$°C) and humidity ($55 \pm 5$%) under a 12-h light/dark cycle and had unlimited access to food and water until the experiment begins.

For the acute, subacute, and high-fat diet (HFD) experiments, mice were anesthetized in an acrylic box filled with 2% isoflurane (RWD, Shenzhen). Hair and scalp were removed. The collimator was anchored to the corresponding surface on the skull using dental cement. The hypothalamus, especially the arcuate nucleus (related to bregma: −1.60 mm anterior/posterior, 0.10 mm medial/lateral, −5.80 mm dorsal/ventral) was the target of ultrasound stimulation while the visual cortex (V1, related to bregma: −2.70 mm anterior/ posterior, 2.50 mm medial/lateral, −0.80 mm dorsal/ventral) was selected as another target to demonstrate the specificity of UDBS. After the dental cement had solidified, the mice were given a week to recover in their home cages.

For the transgenic mice experiment, mice were depilated only on the top of the head to facilitate the ultrasound to reach the target area and to avoid wound infection.

### B. Ultrasound Neuromodulation

Acoustic field simulations were executed with the commercial finite element software COMSOL Multiphysics 6.0 (Comsol Inc., Stockholm, Sweden). The focus ultrasound transducer with a fundamental frequency of 3.8 MHz is attached to the collimator and connected to the head with ultrasound gel. Ultrasound was generated by a two-channel function generator (DG4162, Rigol, Suzhou, China) and a 100 W power amplifier (2100L, EI, NY, USA) and transmitted to the ARC or V1. Needle hydrophone (Precision Acoustics, Dorchester, Dorset, UK) is applied to detect the acoustic pressure distribution inside the skull. Two ultrasound parameters were used in the acute experiment: pulse repetition frequency (PRF) of 500 Hz, duty cycle (DC) of 50%, tone burst duration (TBD) of 1 ms; and PRF of 1.5 kHz, DC of 10%, TBD of 0.067 ms, with sonication duration (SD) of 1 s, inter-stimulus intervals (ISI) of 2 s, and acoustic pressure of 586 kPa. The parameters used in the HFD experiment and the transgenic mice experiment were: PRF of 500 Hz, DC of 50%, TBD of 1 ms, SD of 1 s, ISI of 5 s, and acoustic pressure of 586 kPa.

### C. Acute and Subacute Food Intake

For the acute stimulation experiment, mice were fasted overnight after 48-h acclimatization in the behavioral chamber, followed by the provision of premeasured food in the morning. Mice received ultrasound stimulation in ARC ($n = 8$) or V1 ($n = 7$) for 15 min, followed by measurement of food intake every 30 min for 2 h. The Sham group ($n = 7$) underwent the same process except that the ultrasound output was abolished. The trials were randomized and conducted one week apart on the same animals.

For subacute stimulation experiment, mice were acclimated in the behavioral chamber for 48 hours on an ad libitum diet one week after collimator installation (Day 1 and 2: acclimation period). Premeasured food was then provided and weighed at scheduled time 2 days before (Day 3 and 4: pre-stimulation), 2 days during (Day 5 and 6: UDBS, $n = 8$) and 6 consecutive days after (Day 7 to 12: post-stimulation) ultrasound stimulation. Mice in the Sham group ($n = 5$) performed the experiment with the same protocol, except that a two-day sham stimulation was used instead of ultrasound.

### D. Ultrasound Stimulation of Leptin-Receptor Knockout Mice

Six-week-old BKS-Leprem2Cd479/Gpt (db/db) were randomly divided into two groups ($n = 13$). From Day 2, mice in the UDBS group underwent ultrasound ARC stimulation for 10 days (15 min/day). Six mice in each group were sacrificed after 10-day ultrasound stimulation to collect blood for metabolic assay. The mice were fasted for 4 h before measuring blood glucose levels. The stimulation period lasted 33 days (15 min/d) starting from Day 63. Mice in the Sham group underwent the same procedure except for the absence of ultrasound. The body weight of the mice was measured for the duration of the experiment. Images of leg fat thickness were obtained by the Vevo®2100 ultrasound imaging system (frequency: 40MHz).

### E. Ultrasound Stimulation of Mice Fed a High-Fat Diet

Mice were randomly divided into three groups ($n = 9$). The HFD+UDBS and HFD+Sham groups were provided with a HFD, while the Control group was on a normal diet. Mice were installed with collimators on Day 68. The HFD+UDBS group received ultrasound stimulation for 14 times (15 min/2 days) starting on Day 75, while mice in the HFD+Sham and Control groups underwent the same procedure, except for the absence

of ultrasound. The body weight of mice was monitored and mice were euthanized to collect fat. Images of leg fat thickness were also obtained.

### F. Immunofluorescence

Twelve wild-type mice (n = 6), twelve POMC-CreER::Ai14 mice (n = 6), and eight NPY-CreER::Ai14 mice (n = 4) were randomly divided into two groups, deeply anesthetized 1 h post UDBS or sham treatment and perfused transcardially with 1X phosphate buffer saline (PBS) and 4% paraformaldehyde. The brains were post-fixed with 4% paraformaldehyde overnight, cryoprotected with 30% sucrose for 48 h, then frozen and excised in 30-$\mu$m coronal sections containing the ARC (Leica CM1950, Germany). Brain slices were subsequently incubated for 2 h at room temperature in blocking solution (5% BSA, 1X PBS, 0.25% TritonX100), followed by incubation with rabbit anti-c-Fos anti-body (1:1000, Synaptic System, Germany, #226003) in blocking buffer (1% BSA, 1X PBS, 0.25% TritonX100) for 24 h at 4°C. Slices were rinsed three times with 1X PBS and immersed in blocking buffer with secondary antibody (Alexa Fluor 488-conjugated donkey anti-rabbit IgG, Abcam, USA) at room temperature for 3 h, then washed and mounted on glass slides with fluoromount medium. Images were acquired using a virtual slide microscope (VS200; Olympus, Japan) with a 10x objective.

### G. Metabolic Assay

Blood samples from different groups were collected for metabolic assays employing commercial enzyme-linked immunosorbent assay (ELISA) kits. Serum from each sample was maintained at −20°C for further ELISA assays for triglyceride (TG), cholesterol (CHO), high-density lipoprotein (HDL), low-density lipoprotein (LDL), glucose (GLU) and glycosylated serum protein (GSP). ELISA results were based on wavelength readings (optical density at 405 nm) to evaluate the ELISA ratios (ER).

### H. Electrophysiology

Brains removed from POMC-CreER::Ai14 mice or NPY-CreER::Ai14 mice after experiencing 15 min ultrasound stimulation were quickly submerged in ice-cold oxygenated high sucrose solution (in mM: 60 NaCl, 3 KCl, 7 $MgCl_2$, 1.25 $NaH_2PO_4$, 25 $NaHCO_3$, 10 D-glucose, 115sucrose, and 0.5 $CaCl_2$). Coronal 300 $\mu$m slices containing the ARC were pretreated with Vibratome instrument (VT-1200 Series, Leica) and incubated in the ACSF containing (in mM: 126 NaCl, 2.5 KCl, 1 $MgCl_2$, 1.25 $NaH_2PO_4$, 26 $NaHCO_3$, 10 D-glucose, 2 sodium pyruvate, 0.5 L-ascorbic acid, and 2 $CaCl_2$) for further electrophysiology recording. Using infrared differential interference contrast and fluorescence to observe POMC neurons or NPY neurons. Whole-cell current-clamp recordings were performed using an EPC 10 system (HEKA, Rietberg, Germany) to capture spontaneous action potential firing. Recordings were filtered at 5 kHz and digitized at a 3 kHz sampling rate. The series resistance was compensated, and leakage and capacitive currents were removed online. Patch glass microelectrodes were pulled by micropipette puller (P-97, Sutter Instrument Co., Novato, CA, USA) and the resistance ranged from 5 to 10 MΩ after filling the internal solution. The current-clamp internal solution contained the following (in mM): 140 K-gluconate, 4.5 $MgCl_2$, 5 EGTA, 4 Mg-ATP, 0.3 GTP, 4.4 phosphocreatine disodium salt hydrate, and 9 HEPEs.

### I. Statistical Analysis

SPSS 21.0 statistical software was used in this study. All data were shown as mean ± SEM. The paired-simple t-test was used in the acute and subacute stimulation experiments. One-way analyses of variance (ANOVA) with Tukey's test post hoc test were used in the HFD experiments. The independent sample t-test was used in the remaining experiments. The level of statistical significance was set at $p \leq 0.05$.

## III. Result

### A. UDBS Increases the Expression of c-Fos in the Arcuate Nucleus

Ultrasound transducer was fixed in head and achieved optimal coverage of the hypothalamus by the collimator. Acoustic field simulations were performed for natural ultrasound emission and collimators with different radiuses of departure aperture. The simulated acoustic field distributions and the normalized acoustic pressure along the ultrasound propagation direction are shown in Fig.1 (A-B). The magnitude of the acoustic pressure along the propagation direction was normalized for the above four conditions using the acoustic pressure at the focus without collimator as the standard. The attenuation of the 3 mm radius of the collimator is 60.06%, 84.74% and 96.68% for 3.5 mm and 4 mm, respectively. Considering the safety and reliability of the collimator installation and the size of the mouse skull, 3.5 mm radius collimator was chosen in the subsequent experiments. Fig. 1 (C) shows the photographs of the collimator, ultrasound transducer and assembled together for ultrasound stimulation.

The c-Fos expression is associated with excitatory activity of neurons and is traditionally considered as a marker of neuronal activation. The distribution of acoustic pressure in the brain is shown in Fig. 1 (D), where the acoustic attenuation transmitted through the mouse skull is about 54% (frequency: 3.8 MHz). For wild type mice, the results of immunofluorescence analysis demonstrated that ultrasound stimulation with PRF of 500 Hz, DC of 50%, TBD of 1 ms, SD of 1 s, ISI of 2 s, and acoustic pressure of 586 kPa significantly increased c-Fos expression in the ARC (Sham: 316.93 ± 49.98 /$mm^2$, UDBS: 1071.61 ± 72.37 /$mm^2$, $n = 4$ for Sham group, $n = 6$ for UDBS group, $p < 0.0001$, independent-sample t-test), as shown in Fig. 1 (E) and Fig. 1 (F). All immunofluorescence staining results were shown in Fig. S1.

### B. UDBS Suppresses Acute Food Intake

To test the acute effect of UDBS on feeding, the experiment was conducted following the protocol shown in Fig. 2 (A), with different PRFs ultrasound delivered into the hypothalamus. Fifteen-min UDBS of the hypothalamus with TBD of 1 ms repeated at PRF of 500 Hz decreased the food intake

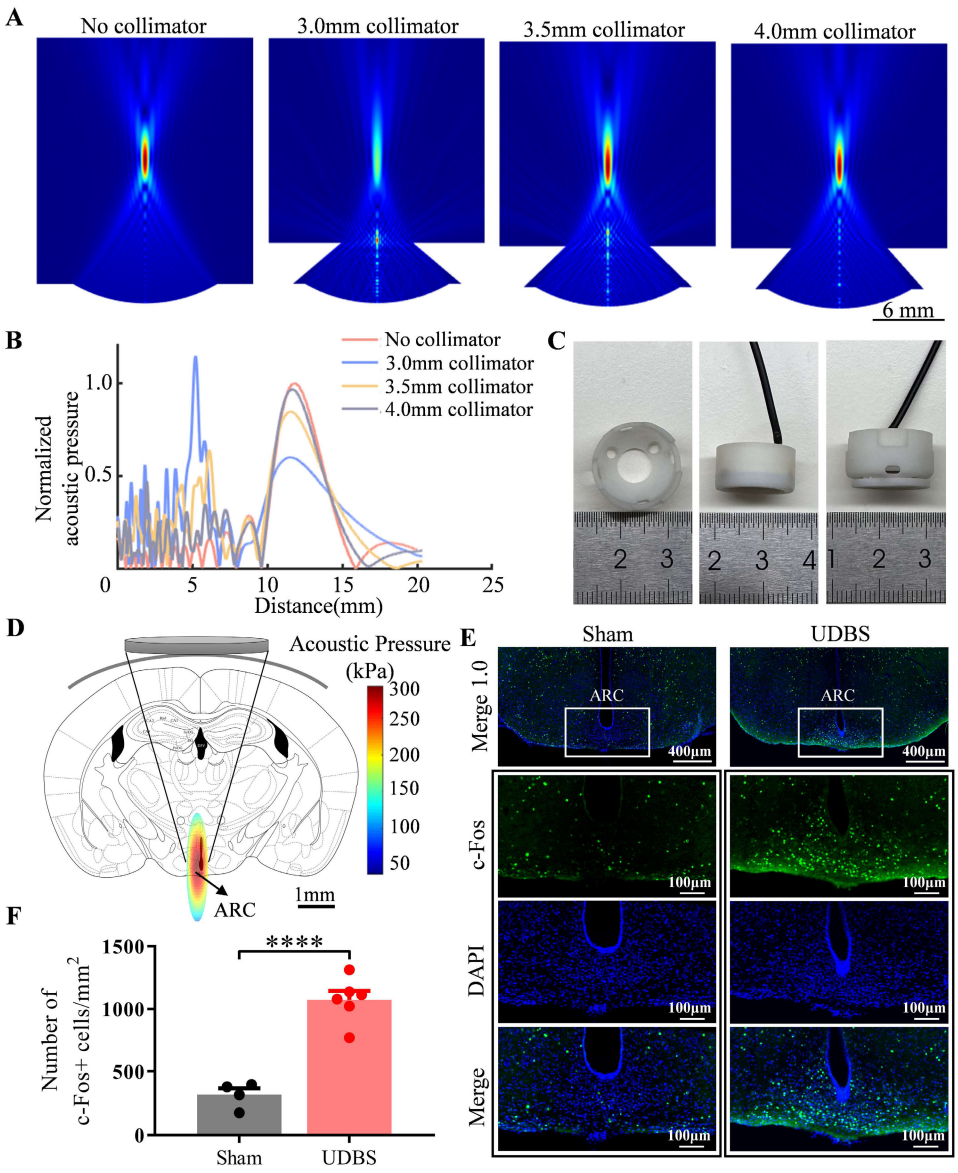


Fig. 1. Simulation of acoustic field of ultrasound transducer and ARC c-Fos abundance after ultrasound stimulation of hypothalamus. (A) The acoustic field simulation of ultrasound emission without collimator and with collimators of different radiuses of departure aperture. (B) The normalized acoustic pressure along the ultrasound propagation direction. (C) Photographs of the actual collimator (left), ultrasound transducer (middle) and their assembly (right) used in the experiment. (D) Stimulation area and acoustic pressure distribution in the coronal plane in the mouse brain. (E) Representative images of c-Fos positive cells (green fluorescence) of the ARC in the Sham and UDBS groups. Cell nuclei were stained by DAPI (blue fluorescence). Scale bar is 400$\mu$m and 100$\mu$m, respectively. (F) Number of c-Fos-positive cells in the Sham and UDBS group. C-Fos-positive cells within the ARC were counted converted to the number contained in 1 mm$^2$ ($n = 6$ for UDBS group, $n = 4$ for Sham group, mean $\pm$ SEM, $****p < 0.0001$, independent-sample t-test).

by 41.4% within 2 h (60 min: Sham: 0.68 $\pm$ 0.05 g, UDBS: 0.47 $\pm$ 0.04 g, $p = 0.0019$; 90 min: Sham: 0.95 $\pm$ 0.06 g, UDBS: 0.57 $\pm$ 0.05 g, $p < 0.0001$; 120 min: Sham: 1.11 $\pm$ 0.08 g, UDBS: 0.65 $\pm$ 0.07 g, $p < 0.0001$; $n = 8$, paired-sample t-test), as shown in Fig. 2 (B). While there were no significant changes in food intake with TBD of 0.067 ms repeated at PRF of 1.5 kHz, as shown in Fig. 2 (C).

The food intake of sham-stimulated mice did not change significantly at all four measured time points, as shown in Fig. 2(D). Furthermore, no significant change in food intake was observed for ultrasound stimulation with TBD of 1 ms and PRF of 500 Hz on V1 that is unrelated to food intake, which excludes the effect of auditory pathway activation, as shown in Fig. S2. The above results indicated that ultrasound needs to specifically stimulate the hypothalamus to control food intake.

### C. UDBS Controls Food Intake in Subacute Experiment

Subacute experiment was subsequently used to verify the long-lasting effect of ultrasound stimulation on appetite suppression, which was performed as shown in Fig. 2 (E). Prolonged 1-hr ultrasound stimulation was able to significantly reduce the daily food intake of mice and the effect lasted for 4 days (Pre-stim: 5.60 $\pm$ 0.17 g, UDBS: 3.27 $\pm$ 0.35 g, Post-stim1: 3.98 $\pm$ 0.39 g, Post-stim2: 4.44 $\pm$ 0.18 g, Post-stim3: 5.01 $\pm$ 0.31 g, Pre-stim *vs.* UDBS: $p = 0.0003$; Pre-stim *vs.* Post-stim1: $p = 0.0048$; Pre-stim *vs.* Post-stim2: $p < 0.0001$; UDBS *vs.* Post-stim1: $p = 0.03$; UDBS *vs.*

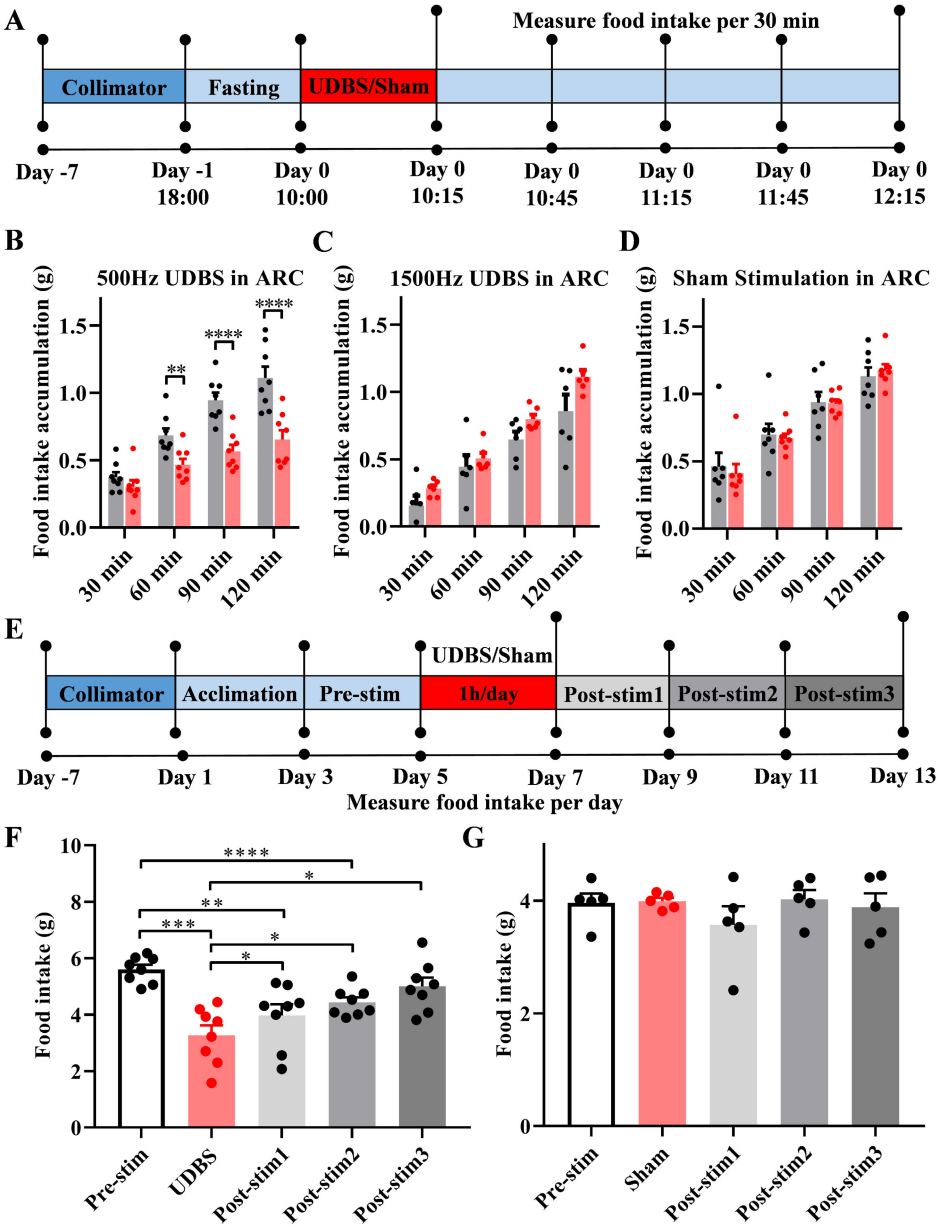


Fig. 2. Ultrasound stimulation suppresses food intake in normal mice. (A) Experimental schedule of acute experiment. Food intake accumulation within 2 h after ultrasound stimulation at PRF of 500 Hz (B) ($n = 8$), at PRF of 1.5 kHz (C) ($n = 6$) and sham stimulation (D) ($n = 7$) compared with that in the previous week (mean ± SEM, $p > 0.05$, $**$ $p < 0.01$, $****$ $p < 0.0001$, paired-sample t-test). (E) Experimental schedule of subacute experiment. Food intake accumulation 2 days before, 2 days during and 6 days after ultrasound stimulation (F) ($n = 8$) and sham stimulation (G) ($n = 5$) (mean ± SEM, $*p < 0.05$, $**$ $p < 0.01$, $***p < 0.001$, $****$ $p < 0.0001$, paired-sample t-test).

Post-stim2: $p = 0.015$; UDBS *vs.* Post-stim3: $p = 0.032$; $n = 8$, paired-sample t-test), whereas sham stimulation of the hypothalamus showed no significant changes in feeding behavior, as shown in Fig. 2 (F-G), demonstrating that UDBS still suppresses appetite for a period of time even after its completion and has a long-lasting effect.

### *D. UDBS Restrains Weight Gain in Leptin-Receptor Knockout Mice*

UDBS of leptin knockout-induced obesity mice (BKS-Leprem2Cd479/Gpt) were performed to verify its effect on body weight regulation, and the protocol was shown in Fig. 3 (A). The first period of UDBS (10 days, 15 min/day) was used to assess the inhibitory effect of ultrasound on weight gain during mouse growth. Body weight gain was 84.89% in the Sham group and 57.98% in the UDBS group until Day 63 (Day 0: Sham: 30.44 ± 0.72 g, UDBS: 28.15 ± 0.88 g; Day 63: Sham: 56.28 ±1.84 g, UDBS: 44.47 ± 2.19 g, $p = 0.0014$, $n = 7$, independent-sample t-test. Detailed data in Table. S1), as shown in Fig. 3 (B) (left). In addition, 10 days of UDBS on the hypothalamus had significantly reduced the growth rate of weight and the effects lasted for at least 51 days (Day 3: Sham: 8.15 ± 0.73%, UDBS: 5.08 ± 1.11%, $p = 0.03$, $n = 13$; Day 63: Sham: 70.86 ± 3.51%, UDBS: 47.10 ± 5.06%, $p = 0.0023$, $n = 7$; independent-sample t-test. Detailed data in Table. S2), as shown in Fig. 3 (B) (right). A second round of ultrasound treatment was performed for one month to

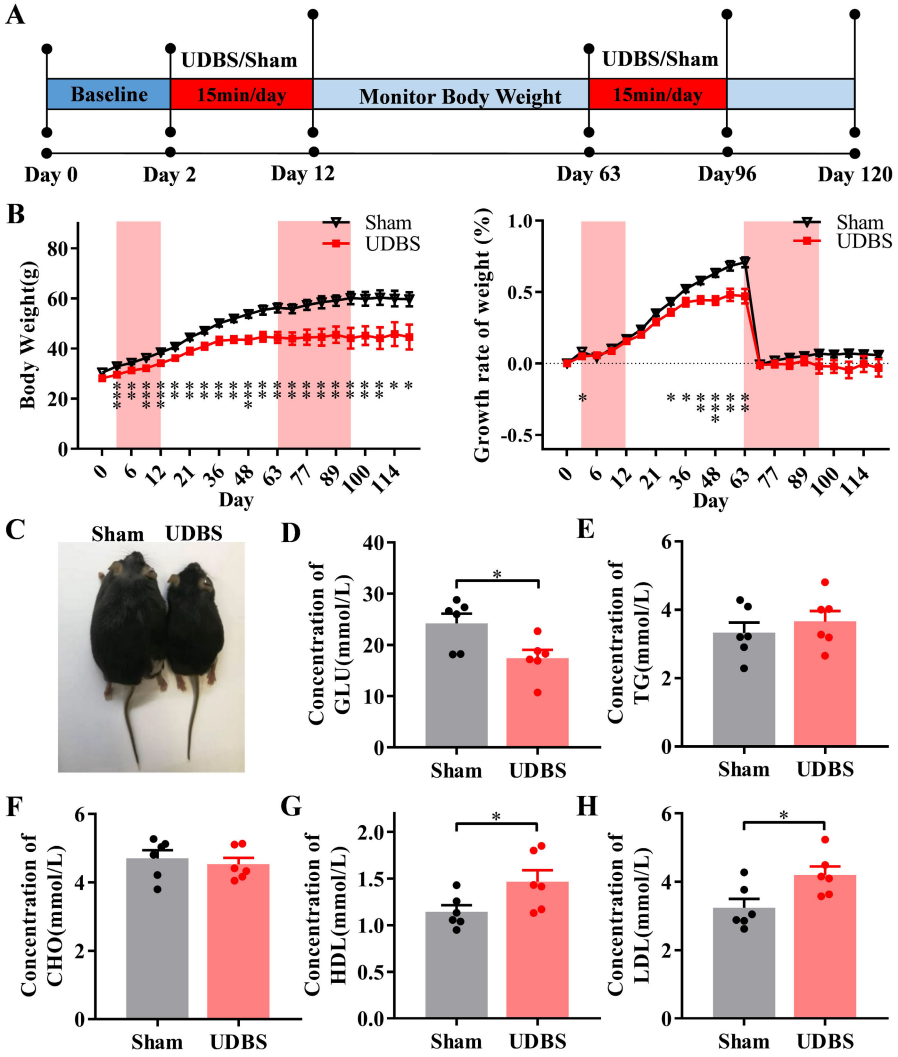


Fig. 3. Ultrasound stimulation controls body weight in transgenic mice lacking leptin receptors. (A) Experimental schedule of ultrasound treatment in transgenic mice lacking leptin receptors. (B) Body weight (left) and growth rate of weight (right) of mice in the Sham and UDBS groups during the whole experiment ( $n = 13$, mean $\pm$ SEM, $p > 0.05$, $*p < 0.05$, $**p < 0.01$, $***p < 0.001$, independent-sample t-test). (C) Representative samples of mice in the Sham and UDBS groups at Day 120. (D–H), Concentration of GLU, TG, CHO, HDL and LDL in the blood of mice in the Sham and UDBS groups ($n = 6$, mean $\pm$ SEM, $p > 0.05$, $*p < 0.05$, independent-sample t-test).

assess the modulating effect of UDBS on body weight in mice with stable body weight. The Sham group gained 6.57% and the UDBS group gained 3.04% during the second-round ultrasound stimulation using the body weight on the first day of the second ultrasound treatment (Day 63) as baseline (Day 120: Sham: 59.72 $\pm$ 2.77 g, UDBS: 44.65 $\pm$ 4.93 g, $p = 0.017$, $n = 7$ for Sham group, $n = 5$ for UDBS group, independent-sample t-test), resulting in a rapid decline in the calculated growth rate of weight. No significant difference in growth rate of weight was observed between the two groups during this period. Comparing the weight of the mice at the beginning and end of the whole experiment, body weight gain was 96.19% in the Sham group and 58.61% in the UDBS group, suggesting that ultrasound treatment had an inhibitory effect on body weight gain in leptin-receptor knockout mice. Photographs of representative mice in Sham and UDBS groups after experiment completion are shown in Fig. 3 (C). The anatomical photographs of mice in both groups are shown in Fig. S3 (A).

The blood results showed that ultrasound stimulation decreased the concentration of GLU, and increased the concentrations of HDL and LDL (GLU: Sham: 24.20 $\pm$ 1.93 mmol/L, UDBS: 17.45 $\pm$ 1.59 mmol/L, $p = 0.02$; HDL: Sham: 1.14 $\pm$ 0.07 mmol/L, UDBS: 1.47 $\pm$ 0.12 mmol/L, $p = 0.048$; LDL: Sham: 3.24 $\pm$ 0.26 mmol/L, UDBS: 4.20 $\pm$ 0.25 mmol/L, $p = 0.025$, $n = 6$, independent-sample t-test), while there was no significant difference between two groups in the concentrations of TG and CHO, as shown in Fig. 3 (D)–3 (H).

The leg fat thickness of the two groups of mice was measured, and the results are shown in Fig. S3 (B) (Sham: 0.86 $\pm$ 0.06 mm, UDBS: 0.83 $\pm$ 0.04 mm, $p = 0.62$, $n = 7$ for Sham group, $n = 6$ for UDBS group, independent-sample t-test).

### E. UDBS Loses Weight in Mice Fed With a High-Fat Diet

The effect of ultrasound on body weight was further verified in normal mice fed a HFD, procedure is shown in Fig. 4 (A). Mice were grouped randomly into three groups: HFD+UDBS,

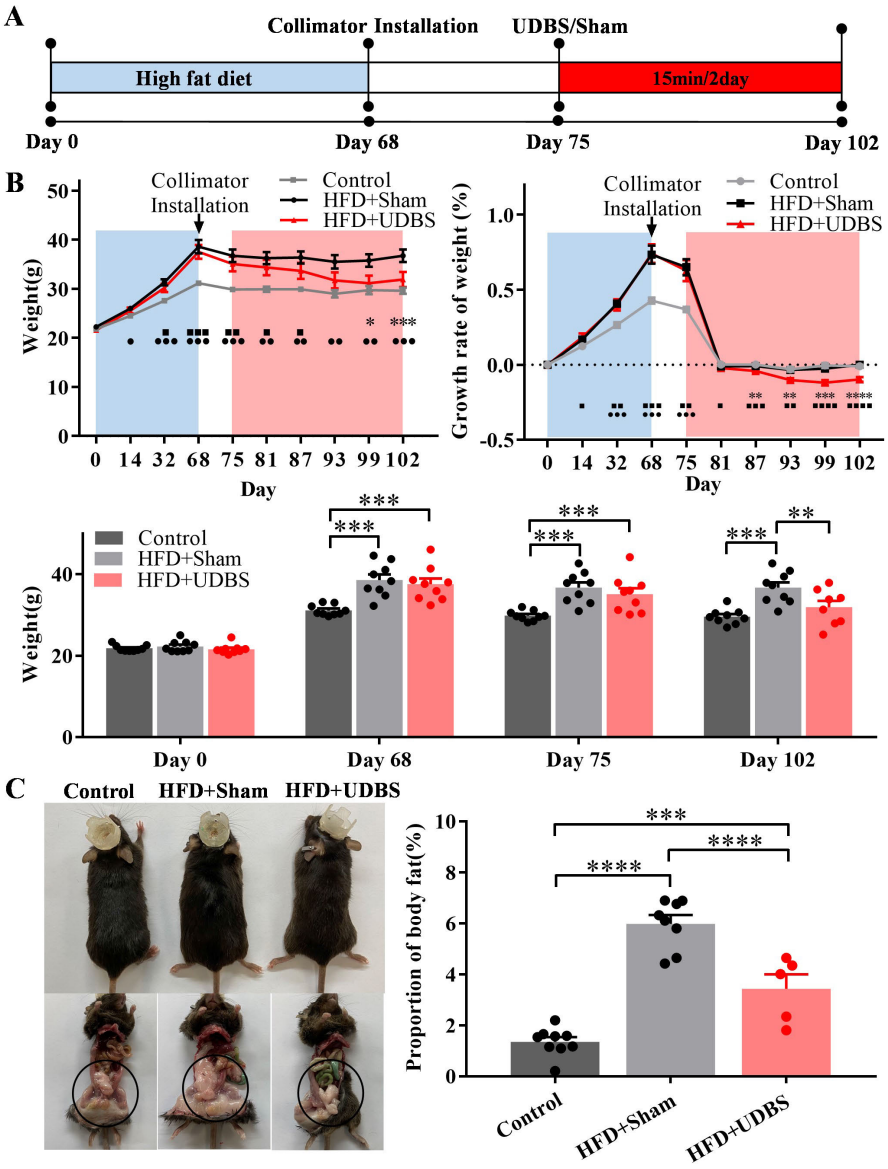


Fig. 4. Ultrasound stimulation of the ARC controls body weight in high-fat diet mice. (A) Experimental schedule of ultrasound stimulation in HFD mice. (B) Body weight (upper left) and growth rate of weight (upper right) of mice in the Control, HFD+Sham and HFD+UDBS groups during the whole experiment. Weight of the Control, HFD+Sham and HFD+UDBS groups at Day 0, Day 68, Day 75, and Day 102 (bottom) ($n = 9$, mean ± SEM, •: Control *vs.* HFD+Sham, ■: Control *vs.* HFD+UDBS, *: HFD+Sham *vs.* HFD+UDBS, one-way ANOVA). (C) Representative samples of mice (left) and proportion of body fat (right) in the Control, the HFD+Sham and UDBS groups at Day 102 ($n = 9$ for Control group, $n = 8$ for Sham group, $n = 5$ for the UDBS group, mean ± SEM, one-way ANOVA).

HFD+Sham and Control groups. The weights of all groups of mice were monitored, as shown in Fig. 4 (B). Until Day 68, the body weight of mice in the Control group increased by 42.71%, and the HFD+Sham and HFD+UDBS groups increased 73.28% and 74.05% respectively, which showed that the body weight of mice with HFD was significantly higher than that of mice fed with normal diet (Day 0: Control: 21.82 ± 0.26 g, HFD+Sham: 22.27 ± 0.45 g, HFD+UDBS: 21.58 ± 0.40 g; Day 68: Control: 31.14 ± 0.44 g, HFD+Sham: 38.59 ± 1.37 g, HFD+UDBS: 37.56 ± 1.41 g, Control *vs.* HFD+Sham: $p = 0.0001$, Control *vs.* HFD+UDBS: $p = 0.0007$, $n$= 9, one-way ANOVA). We also analyzed the growth rate of weight, which showed that the Sham and HFD UDBS groups were essentially the same before UDBS treatment and were significantly higher than that of the Control group, which was caused by the HFD. After 4 weeks of UDBS (15 min/ 2 days) were given to the HDF+UDBS group, body weight gain was −0.90% in the Control group, 0 % in the HFD+Sham group, and -9.09 % in the HFD+UDBS group compared with the data at the beginning of the stimulation (Day 75) (Day 75: Control: 29.86 ± 0.41 g, HFD+Sham: 36.73 ± 1.28 g, HFD+UDBS: 35.08 ± 1.50 g, Control *vs.* HFD+Sham: $p = 0.0003$, Control *vs.* HFD+UDBS: $p = 0.004$; Day 102: Control: 29.59 ± 0.62 g, HFD+Sham: 36.73 ± 1.30 g, HFD+UDBS: 31.89 ± 1.57 g, Control *vs.* HFD+Sham: $p = 0.0003$, HFD+Sham *vs.*HFD+UDBS: $p = 0.0097$; $n = 9$, one-way ANOVA, Detailed data in Table. S3). The growth rate of weight was significantly lower in the HFD+UDBS group than in the HFD+Sham and Control groups during ultrasound stimulation

using the body weight on the day UDBS initiation as the baseline (Day 81: Control: -0.14 ± 0.77 %, HFD+Sham: 1.19 ± 0.71 %, HFD+UDBS: -2.17 ± 0.78 %, Control *vs.* HFD+UDBS: $p = 0.04$; Day 102: Control: -0.94 ± 0.95 %, HFD+Sham: 0.00 ± 0.69 %, HFD+UDBS: -9.75 ± 1.59 %, Control *vs.* HFD+UDBS: $p < 0.0001$, HFD+Sham *vs.* HFD+UDBS: $p < 0.0001$, $n = 9$, one-way ANOVA; detailed data in Table. S4), as shown in Fig. 4 (B). Compared to the data at Day 0, the body weight had increased by 35.61% in the Control group, 64.93% in the HFD+Sham group, and 47.78% in the HFD+UDBS group, which indicated that the weight of the HFD+UDBS group decreased significantly after ultrasound treatment compared with the HFD+Sham group, and weight difference between the HFD+UDBS and Control groups with normal diet gradually decreased to nonsignificant during the UBDS period. These results indicate that ultrasound stimulation can significantly inhibit the weight gain of HFD mice to restore the normal level and also achieve weight loss.

Fig. 4 (C) shows the representative photographs (left) of mice in the Control, Sham, and UDBS groups after the experiment. The proportion of body fat in HFD+UDBS was significantly decreased after ultrasound stimulation when compared to the HFD+Sham group (Control: 1.35 ± 0.18 %, HFD+Sham: 5.98 ± 0.34 %, HFD+UDBS: 3.43 ± 0.57 %, Control *vs.*HFD+Sham: $p < 0.0001$, Control *vs.*HFD+UDBS: $p = 0.0006$, HFD+Sham *vs.* HFD+UDBS: $p < 0.0001$, $n = 9$ for Control group, $n = 8$ for HFD+Sham group, $n = 5$ for HFD+UDBS group, one-way ANOVA), as shown in Fig. 4 (C)(right). The leg fat thickness of mice was also measured, and the results are shown in Fig. S4 (Control: 0.39 ± 0.03 mm, HFD+Sham: 0.50 ± 0.04 mm, HFD+UDBS: 0.47 ± 0.03 mm, Control *vs.* HFD+Sham: $p = 0.04$, $n = 8$, one-way ANOVA).

### *F. Ultrasound Controls Food Intake and Body Weight Through Activation of POMC Neurons*

There are two major neurons in the ARC, the POMC neuron that expresses pro-aponeurotic melanocortin and the NPY/AgRP neurons that express the neuropeptide Y (NPY) and agouti-related protein (AgRP), which play an important role in the regulation of body weight. The population of neuronal cells activated by ultrasound was identified by c-Fos immunostaining and the possible colocalization with either POMC-positive neurons or NYP-positive neurons using POMC-CreER::Ai14 mice and NPY-CreER::Ai14 mice, respectively. Representative immunofluorescence staining results are shown in Fig. 5 (A) (top) and Fig. 5 (B) (top). There was a significant increase in colocalization of c-Fos and POMC-co-positive cells between the Sham and UDBS groups (Sham: 96.00 ± 35.50 /mm$^2$, UDBS: 239.05 ± 45.08 /mm$^2$, $p = 0.04$, $n = 5$ for Sham group, $n = 7$ for UDBS group, independent-sample t-test), as shown in Fig. 5 (A) (bottom). In contrast, there was no significant difference in colocalization of c-Fos- and NPY-co-positive cells between two groups, as shown in Fig. 5 (B) (bottom). Moreover, we examined the neural activity of POMC or NPY neurons in mice which received 15 min UDBS of ARC region (Fig. 5 (C)). The spontaneous action potentials firing frequency of POMC neurons was significantly increased after 15 min UDBS compared to the Sham group (Sham: 1.24 ± 0.13 Hz, UDBS: 1.82 ± 0.12 Hz, $p = 0.004$, $n = 6$ for Sham group, $n = 8$ for UDBS group, independent-sample t-test), as shown in Fig.5 (D) (top), whereas no significant changes were observed in NPY neurons, as shown in Fig.5 (D) (bottom). Thus, we propose that ultrasound-induced activation of POMC neurons may be one of the prime reasons for the suppression of feeding and weight gain, as summarized in Fig. 6.

## IV. Discussion

We developed a noninvasive neuromodulation technique for the control of food intake and body weight in mice, which reduced food intake by 41.4% in acute treatment (Fig. 2) and weight gain by more than 28% in long-term treatment (Fig. 4). Previous study indicated that fifteen days of DBS treatment resulted in approximately 15% reduction in food intake and less than 5% difference in body weight [36]. Optogenetic activation of $CCK^{NTS}$ neuron neurons reduces food intake by no more than 30% and body weight by about 12% [37]. Compared to other physical neuromodulation tools, ultrasound neuromodulation technique is able to deliver energy noninvasively to the deep brain nuclei without adverse effects, does not rely on genetic modification of cells and tissues, and can be used in larger animals and humans. These advantages present the potential for exploring deep-brain targets using ultrasound as a tool for interventions and treatment of brain disorders, and UDBS appears to be a promising therapeutic option for the control of food intake and body weight.

The long-lasting effects of ultrasound stimulation were observed in our study. Ultrasound stimulation of hypothalamus for 2 days (1 h / day) resulted in significant reduction in food intake for 4 days (Fig. 2). Ultrasound stimulation for 10 consecutive days (15 min / day) inhibited weight gain in leptin-receptor knockout (Fig. 3). Ultrasound stimulation 14 times (15 min every two days) similarly caused weight loss in mice on HFD (Fig. 4). We previously found the long lasting effect of 30-min ultrasound stimulation in Parkinson's disease model mice remained after 6 hours in the pole test [17], and 10 consecutive days (10 min / day) of ultrasound treatment increased dendritic spine density and brain plasticity [17]. Twenty minutes of ultrasound stimulation improved sensorimotor performance in animals with ischemic stroke and lasted for four weeks [38]. Functional connectivity in primates changed for more than 1 h after 40 seconds of ultrasound treatment [39]. These findings suggest that ultrasound may be a potent neuromodulation modality and its potential for therapeutic application is encouraging.

The arcuate nucleus includes several important and diverse populations of neurons that mediate different neuroendocrine and physiological functions, including neuroendocrine neurons, centrally projecting neurons, and astrocytes [40]. Different neuroendocrine neurons secrete various types or combinations of neurotransmitters and neuropeptides. The neuroendocrine neurons include POMC neurons, NPY neurons, gonadotropin-releasing hormone neurons, growth hormone–releasing hormone, tuberoinfundibular dopamine neurons, and kisspeptin/NKB neurons. Centrally-projecting

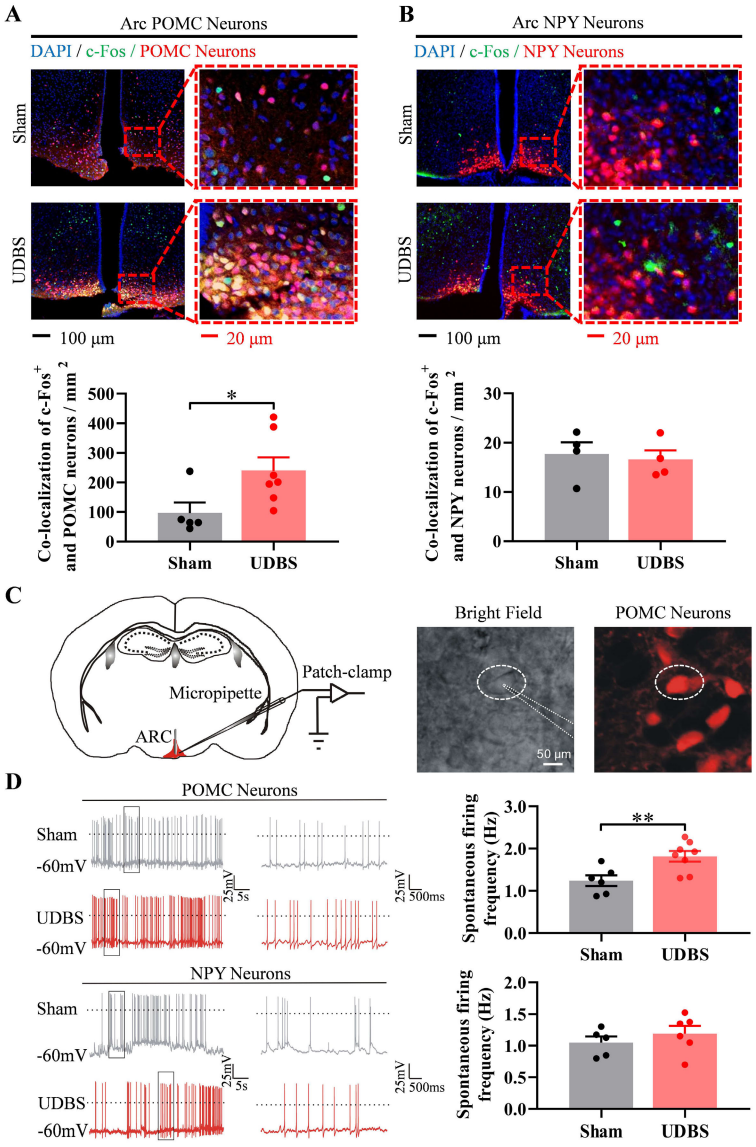


Fig. 5. Ultrasound stimulation of the hypothalamus activated POMC neurons in ARC. Representative images and statistical diagram of co-located cells with c-Fos and POMC neurons (A) ($n = 5$ for Sham group, $n = 7$ for UDBS group) or c-Fos and NPY neurons (B) ($n = 4$) in the ARC of the Sham and the UDBS groups (mean ± SEM, $*p < 0.05$, independent-sample t-test). Ultrasound increases colocalization of c-Fos–positive cells with POMC-positive cells in the ARC. (C) Schematic diagram of electrophysiological recording in POMC neurons of the ARC region. (D) Representative traces of spontaneous action potential firing and statistical graphs of neuronal activity of POMC neurons (top) ($n = 6$ for Sham group, $n = 8$ for UDBS group, mean ± SEM, $**p < 0.01$, independent-sample t-test) and NPY neurons (bottom) ($n = 5$ for Sham group, $n = 6$ for UDBS group, mean ± SEM, independent-sample t-test).

neurons have projection pathways from the arcuate nucleus to mediate different regions of the brain, such as the amygdala, entorhinal cortex, dorsomedial hypothalamic nucleus, lateral hypothalamus and paraventricular nucleus of the hypothalamus which are important in the regulation of appetite [41]. Many studies have shown that POMC and NPY neurons are crucial in regulating energy metabolism [6], [42], [43], [44], [45]. Chemogenetic and optogenetic techniques activate POMC neurons to inhibit food intake and body weight loss [6], [46], [47], [48], [49], [50], [51], [52], [53]. The feeding system will be unbalanced and prone to obesity when POMC neurons are damaged [54]. Similar experiments on NPY neurons have shown that activating NPY neurons can promote feeding [46], while destroying them can cause anorexia, weight loss and even death [55]. We therefore investigated the activities of POMC and NPY neurons induced by ultrasound. Our immunofluorescence and electrophysiology results showed that ultrasound-induced suppression of food intake was accompanied by an increase in POMC neuron activation, which may be one of the potential contributors to the effect of weight loss. The underlying mechanisms involved in UDBS control of food intake may be the regulation in activities of POMC neurons (Fig. 6). However, there are now also studies finding that chronic inhibition of NPY neurons and chronic activation of POMC neurons have no effect on body weight [56], [57]. It has been also found that acute activation of POMC neurons in the ARC fails to suppress food intake, whereas chronic activation reduced body weight and

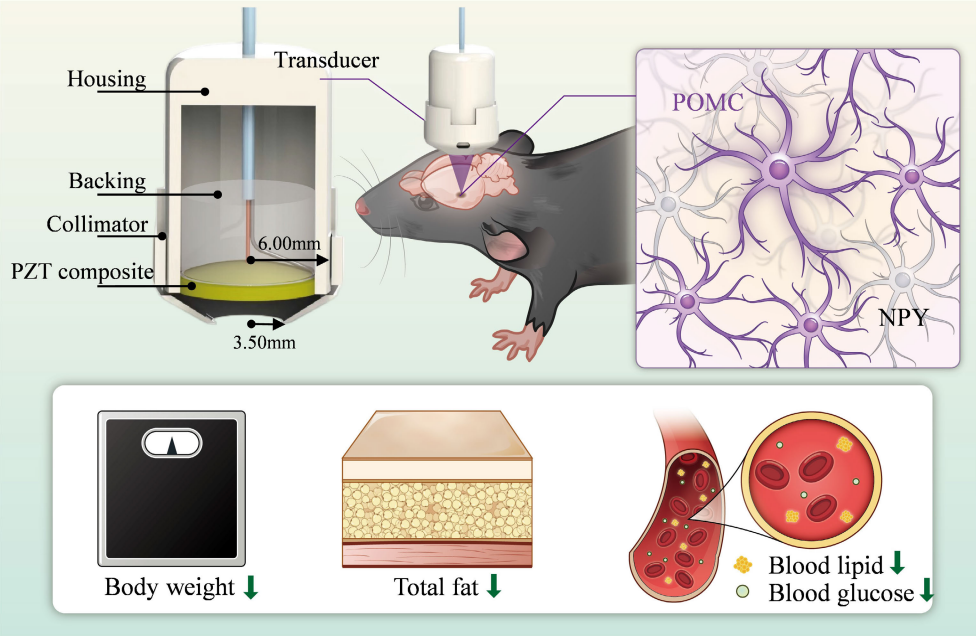


Fig. 6. Schematic representation of the ultrasound deep brain stimulation control of body weight.

food intake [47]. However, several studies have demonstrated that activation of POMC neurons can reduce food intake through localized leptin administration, nicotine treatment, or adiponectin [43], [58], [59]. Thus, there is a significant connection between activation of POMC neurons in ARC and reduction in feeding behavior. The possible reasons for the inconsistent results are related to the changes in the stimulation modalities and protocols.

Despite the fact that the mechanisms of ultrasound neuromodulation are completely unclear, it has been demonstrated that acoustic radiation forces induce neuronal activities by modulation of mechanosensitive ion channels [60], [61], [62], [63], [64]. Therefore, we hypothesized that acoustic radiation force modulated mechanosensitive ion channels of POMC neurons to active POMC neurons in our study. Furthermore, previous studies in a theoretical model [65], *in vitro* [62] and *in vivo* [66] experiments have shown feasibility of cell-type-specific effects induced by ultrasound. Specific ultrasound parameter set selectively increases the activity of parvalbumin interneurons while inhibiting excitatory neurons in the hippocampus and obtains significant spike inhibition in the kainate model of chronic temporal lobe epilepsy [67]. The differences in response to ultrasound observed in different cell types may be attributed to the types and relative distributions of ion channels in each neuron-type and/or the distinct shape and orientation of the axonal and dendritic arbors, and the discharge frequency of neurons. Thus, the selection of appropriate ultrasound parameters is essential since it can result in different response profiles of different types of neurons to the dynamic acoustic radiation force applied by PRFs [66].

Two studies demonstrated that activation of indirect auditory system led to ultrasound-induced cortical activity and movement [68], [69]. However, ultrasound stimulation directly activates neurons in brain slices [29], [70], [71], retina [72] and C. elegans [63], [73] independent of the auditory transmission pathway. Visual cortex as a stimulation target of UDBS fails to modulate motor function in mice [17], [25], [74]. Importantly, the modulation effect of ultrasound on hearing impaired mice is consistent with that of normal mice and is not inhibited by deafness [75]. In this study, UDBS of the primary visual cortex did not affect food intake in fasted mice (Fig. S2). These results suggest that ultrasound-induced behavioral responses directly activate the nuclei rather than indirect activation through the auditory pathways. In addition, many studies have investigated the side effects of ultrasound neuromodulation. Several subjects reported mild to moderate level of symptoms, including neck pain, sleepiness, muscle twitches, itchiness and headache, but all of them were transient in 20 follow-up participants [76], while a case suffered transient headache after the sham TUS session in a total of 19 healthy volunteers [77]. He et al. reported that ultrasound did not cause adverse effects such as headache or anxiety in patients, but some individuals had scalp tingling sensation at specific parameters. However, no side effects have been reported in most of the human studies [19], [78], [79]. In the 120-person experiment with 64 participants who attended follow-up, only seven reported mild to moderate symptoms including neck pain, attention problems, muscle twitching, and anxiety, with no serious adverse effects in any participant. The characterization and incidence of symptoms appeared similar to other forms of noninvasive brain stimulation [80]. We also did not observe any negative effects in mice during the experiment and confirmed that UDBS did not cause motor or mental disorders in mice (Fig. S5).

Neuromodulation of obesity is an emerging and promising tool for investigating and curing related brain abnormalities, but it is still in its infancy. Therapeutic studies of ultrasound stimulation are even more lacking, and our results confirmed that it is a safe, effective, and low-cost treatment method. However, the small size of the focused ultrasound transducer in this experiment is not suitable for future applications in the clinical treatment of obese patients, phased array ultrasound

transducer with low frequency might be available to reduce acoustic attenuation and meet the individual characteristics. Refinements in ultrasound stimulation parameters applicable to humans are also imperative for future clinical studies and treatments. Future research should also emphasize the formulation of optimal ultrasound stimulation target according to the patient's obesity phenotype for personalized medicine.

## V. Conclusion

UDBS of hypothalamus could modulate food intake and body weight in normal mice, leptin receptor knockout mice, and high-fat fed mice. UDBS appears to achieve its regulatory effect by activating POMC neurons. To summarize, a conceptual proof is provided that UDBS of the hypothalamus can operate as a non-invasive neuromodulation tool to regulate food intake and body weight, and may as a new strategy for treatment of obesity.

## Acknowledgment

The authors would like to thank J. Hu from Shanghai Tech University, N. Li from Qingdao University, L. Li from Shenzhen Institutes of Advanced Technology, Chinese Academy of Sciences, and B. Peng from Fudan University for POMC-CreER::Ai14 mice and NPY- CreER::Ai14 transgenic mice and helpful comments.

## References

[1] P. G. Kopelman, "Obesity as a medical problem," *Nature*, vol. 404, no. 6778, pp. 635–643, Apr. 2000.

[2] C. L. Ogden, M. D. Carroll, L. R. Curtin, M. A. McDowell, C. J. Tabak, and K. M. Flegal, "Prevalence of overweight and obesity in the United States, 1999–2004," *J. Amer. Med. Assoc.*, vol. 295, no. 13, pp. 1549–1555, 2006.

[3] A. Afshin et al., "Health effects of overweight and obesity in 195 countries over 25 years," *New England J. Med.*, vol. 377, no. 1, pp. 13–27, 2017.

[4] T. Lung, S. Jan, E. J. Tan, A. Killedar, and A. Hayes, "Impact of overweight, obesity and severe obesity on life expectancy of Australian adults," *Int. J. Obesity*, vol. 43, no. 4, pp. 782–789, Apr. 2019.

[5] P. Abelson and D. Kennedy, "The obesity epidemic," *Science*, vol. 304, no. 5676, p. 1413, 2004.

[6] M. A. Cowley et al., "Leptin activates anorexigenic POMC neurons through a neural network in the arcuate nucleus," *Nature*, vol. 411, no. 6836, pp. 480–484, May 2001.

[7] A. R. C. Barreto-Vianna, M. B. Aguila, and C. A. Mandarim-de-Lacerda, "Effects of liraglutide in hypothalamic arcuate nucleus of obese mice," *Obesity*, vol. 24, no. 3, pp. 626–633, Mar. 2016.

[8] A. M. Herman et al., "A cholinergic basal forebrain feeding circuit modulates appetite suppression," *Nature*, vol. 538, no. 7624, pp. 253–256, Oct. 2016.

[9] C. H. Göbel, V. M. Tronnier, and T. F. Munte, "Brain stimulation in obesity," *Int. J. Obesity*, vol. 41, no. 12, pp. 1721–1727, Dec. 2017.

[10] D. A. Formolo et al., "Deep brain stimulation for obesity: A review and future directions," *Frontiers Neurosci.*, vol. 13, p. 323, Apr. 2019.

[11] C. C. Nestor et al., "Optogenetic stimulation of arcuate nucleus Kiss1 neurons reveals a steroid-dependent glutamatergic input to POMC and AgRP neurons in male mice," *Mol. Endocrinol.*, vol. 30, no. 6, pp. 630–644, Jun. 2016.

[12] X. Zhang and A. N. van den Pol, "Hypothalamic arcuate nucleus tyrosine hydroxylase neurons play orexigenic role in energy homeostasis," *Nature Neurosci.*, vol. 19, no. 10, pp. 1341–1347, Oct. 2016.

[13] W. Legon et al., "Transcranial focused ultrasound modulates the activity of primary somatosensory cortex in humans," *Nature Neurosci.*, vol. 17, no. 2, pp. 322–329, 2014.

[14] D. Folloni et al., "Manipulation of subcortical and deep cortical activity in the primate brain using transcranial focused ultrasound stimulation," *Neuron*, vol. 101, no. 6, pp. 1109–1116, Mar. 2019.

[15] E. F. Fouragnan et al., "The macaque anterior cingulate cortex translates counterfactual choice value into actual behavioral change," *Nature Neurosci.*, vol. 22, no. 5, pp. 797–808, May 2019.

[16] Y. Tufail et al., "Transcranial pulsed ultrasound stimulates intact brain circuits," *Neuron*, vol. 66, no. 5, pp. 681–694, Jun. 2010.

[17] H. Zhou et al., "Noninvasive ultrasound deep brain stimulation for the treatment of Parkinson's disease model mouse," *Research*, vol. 2019, Jan. 2019, Art. no. 1748489.

[18] J. Mueller, W. Legon, A. Opitz, T. F. Sato, and W. J. Tyler, "Transcranial focused ultrasound modulates intrinsic and evoked EEG dynamics," *Brain Stimulation*, vol. 7, no. 6, pp. 900–908, Nov. 2014.

[19] W. Lee, Y. A. Chung, Y. Jung, I.-U. Song, and S.-S. Yoo, "Simultaneous acoustic stimulation of human primary and secondary somatosensory cortices using transcranial focused ultrasound," *BMC Neurosci.*, vol. 17, no. 1, p. 68, Dec. 2016.

[20] W. Legon, L. Ai, P. Bansal, and J. K. Mueller, "Neuromodulation with single-element transcranial focused ultrasound in human thalamus," *Hum. Brain Mapping*, vol. 39, no. 5, pp. 1995–2006, May 2018.

[21] N. Pang et al., "Ultrasound deep brain stimulation modulates body temperature in mice," *IEEE Trans. Neural Syst. Rehabil. Eng.*, vol. 30, pp. 1851–1857, 2022.

[22] T. Guo et al., "Pulsed transcranial ultrasound stimulation immediately after the ischemic brain injury is neuroprotective," *IEEE Trans. Biomed. Eng.*, vol. 62, no. 10, pp. 2352–2357, Oct. 2015.

[23] L. Liu et al., "Protective effect of low-intensity transcranial ultrasound stimulation after differing delay following an acute ischemic stroke," *Brain Res. Bull.*, vol. 146, pp. 22–27, Mar. 2019.

[24] H. Baek, A. Sariev, S. Lee, S.-Y. Dong, S. Royer, and H. Kim, "Deep cerebellar low-intensity focused ultrasound stimulation restores interhemispheric balance after ischemic stroke in mice," *IEEE Trans. Neural Syst. Rehabil. Eng.*, vol. 28, no. 9, pp. 2073–2079, Sep. 2020.

[25] T. Bian et al., "Noninvasive ultrasound stimulation of ventral tegmental area induces reanimation from general anaesthesia in mice," *Research*, vol. 2021, Jan. 2021, Art. no. 2674692.

[26] B.-K. Min et al., "Focused ultrasound-mediated suppression of chemically-induced acute epileptic EEG activity," *BMC Neurosci.*, vol. 12, no. 1, p. 23, Dec. 2011.

[27] H. Hakimova, S. Kim, K. Chu, S. K. Lee, B. Jeong, and D. Jeon, "Ultrasound stimulation inhibits recurrent seizures and improves behavioral outcome in an experimental model of mesial temporal lobe epilepsy," *Epilepsy Behav.*, vol. 49, pp. 26–32, Aug. 2015.

[28] X. Li, H. Yang, J. Yan, X. Wang, X. Li, and Y. Yuan, "Low-intensity pulsed ultrasound stimulation modulates the nonlinear dynamics of local field potentials in temporal lobe epilepsy," *Frontiers Neurosci.*, vol. 13, p. 287, Apr. 2019.

[29] Z. Lin et al., "Non-invasive ultrasonic neuromodulation of neuronal excitability for treatment of epilepsy," *Theranostics*, vol. 10, no. 12, pp. 5514–5526, 2020.

[30] J. Zou et al., "Ultrasound neuromodulation inhibits seizures in acute epileptic monkeys," *iScience*, vol. 23, no. 5, May 2020, Art. no. 101066.

[31] H. Zhou et al., "Wearable ultrasound improves motor function in an MPTP mouse model of Parkinson's disease," *IEEE Trans. Biomed. Eng.*, vol. 66, no. 11, pp. 3006–3013, Nov. 2019.

[32] H. Zhou et al., "Transcranial ultrasound stimulation suppresses neuroinflammation in a chronic mouse model of Parkinson's disease," *IEEE Trans. Biomed. Eng.*, vol. 68, no. 11, pp. 3375–3387, Nov. 2021.

[33] Y. Yuan, Z. Zhao, Z. Wang, X. Wang, J. Yan, and X. Li, "The effect of low-intensity transcranial ultrasound stimulation on behavior in a mouse model of Parkinson's disease induced by MPTP," *IEEE Trans. Neural Syst. Rehabil. Eng.*, vol. 28, no. 4, pp. 1017–1021, Apr. 2020.

[34] R. Beisteiner et al., "Transcranial pulse stimulation with ultrasound in Alzheimer's disease—A new navigated focal brain therapy," *Adv. Sci.*, vol. 7, no. 3, Feb. 2020, Art. no. 1902583.

[35] J. A. Cain et al., "Ultrasonic deep brain neuromodulation in acute disorders of consciousness: A proof-of-concept," *Brain Sci.*, vol. 12, no. 4, p. 428, Mar. 2022.

[36] M. L. Soto-Montenegro, J. Pascau, and M. Desco, "Response to deep brain stimulation in the lateral hypothalamic area in a rat model of obesity: In vivo assessment of brain glucose metabolism," *Mol. Imag. Biol.*, vol. 16, no. 6, pp. 830–837, Dec. 2014.

[37] G. D'Agostino et al., "Appetite controlled by a cholecystokinin nucleus of the solitary tract to hypothalamus neurocircuit," *eLife*, vol. 5, p. e12225, Mar. 2016.

[38] H. Baek, K. J. Pahk, M.-J. Kim, I. Youn, and H. Kim, "Modulation of cerebellar cortical plasticity using low-intensity focused ultrasound for poststroke sensorimotor function recovery," *Neurorehabilitation Neural Repair*, vol. 32, no. 9, pp. 777–787, Sep. 2018.

[39] L. Verhagen et al., "Offline impact of transcranial focused ultrasound on cortical activation in primates," *eLife*, vol. 8, p. e40541, Feb. 2019.

[40] J. N. Campbell et al., "A molecular census of arcuate hypothalamus and median eminence cell types," *Nature Neurosci.*, vol. 20, no. 3, pp. 484–496, Mar. 2017.

[41] S. G. Bouret, S. J. Draper, and R. B. Simerly, "Formation of projection pathways from the arcuate nucleus of the hypothalamus to hypothalamic regions implicated in the neural control of feeding behavior in mice," *J. Neurosci.*, vol. 24, no. 11, pp. 2797–2805, 2004.

[42] C. F. Elias et al., "Leptin differentially regulates NPY and POMC neurons projecting to the lateral hypothalamic area," *Neuron*, vol. 23, no. 4, pp. 775–786, Aug. 1999.

[43] S. Suyama, F. Maekawa, Y. Maejima, N. Kubota, T. Kadowaki, and T. Yada, "Glucose level determines excitatory or inhibitory effects of adiponectin on arcuate POMC neuron activity and feeding," *Sci. Rep.*, vol. 6, no. 1, p. 30796, Aug. 2016.

[44] M. Koch et al., "Hypothalamic POMC neurons promote cannabinoid-induced feeding," *Nature*, vol. 519, no. 7541, pp. 45–50, Mar. 2015.

[45] L. Zhang, D. Hernandez-Sanchez, and H. Herzog, "Regulation of feeding-related behaviors by arcuate neuropeptide Y neurons," *Endocrinology*, vol. 160, no. 6, pp. 1411–1420, 2019.

[46] Y. Aponte, D. Atasoy, and S. M. Sternson, "AGRP neurons are sufficient to orchestrate feeding behavior rapidly and without training," *Nature Neurosci.*, vol. 14, no. 3, pp. 351–355, Mar. 2011.

[47] C. Zhan et al., "Acute and long-term suppression of feeding behavior by POMC neurons in the brainstem and hypothalamus, respectively," *J. Neurosci.*, vol. 33, no. 8, pp. 3624–3632, Feb. 2013.

[48] W. Fan, B. A. Boston, R. A. Kesterson, V. J. Hruby, and R. D. Cone, "Role of melanocortinergic neurons in feeding and the agouti obesity syndrome," *Nature*, vol. 385, no. 6612, pp. 165–168, Jan. 1997.

[49] H. M. Hsiung et al., "A novel and selective $\beta$-melanocyte-stimulating hormone-derived peptide agonist for melanocortin 4 receptor potently decreased food intake and body weight gain in diet-induced obese rats," *Endocrinology*, vol. 146, no. 12, pp. 5257–5266, Dec. 2005.

[50] J. E. Mcminn, C. W. Wilkinson, P. J. Havel, S. C. Woods, and M. W. Schwartz, "Effect of intracerebroventricular $\alpha$-MSH on food intake, adiposity, c-Fos induction, and neuropeptide expression," *Amer. J. Physiol.-Regulatory, Integrative Comparative Physiol.*, vol. 279, no. 2, pp. 695–703, Aug. 2000.

[51] M. M. Ollmann et al., "Antagonism of central melanocortin receptors in vitro and in vivo by agouti-related protein," *Science*, vol. 278, no. 5335, pp. 135–138, Oct. 1997.

[52] M. J. Metz, C. M. Daimon, C. M. King, A. R. Rau, and S. T. Hentges, "Individual arcuate nucleus proopiomelanocortin neurons project to select target sites," *Amer. J. Physiol.-Regulatory, Integrative Comparative Physiol.*, vol. 321, no. 6, pp. 982–989, Dec. 2021.

[53] M. Trotta et al., "Hypothalamic Pomc expression restricted to GABAergic neurons suppresses Npy overexpression and restores food intake in obese mice," *Mol. Metabolism*, vol. 37, Jul. 2020, Art. no. 100985.

[54] M. Schneeberger et al., "Mitofusin 2 in POMC neurons connects ER stress with leptin resistance and energy imbalance," *Cell*, vol. 155, no. 1, pp. 172–187, Sep. 2013.

[55] Q. Wu, M. P. Boyle, and R. D. Palmiter, "Loss of GABAergic signaling by AgRP neurons to the parabrachial nucleus leads to starvation," *Cell*, vol. 137, no. 7, pp. 1225–1234, Jun. 2009.

[56] C. Zhu et al., "Profound and redundant functions of arcuate neurons in obesity development," *Nature Metabolism*, vol. 2, no. 8, pp. 763–774, Jul. 2020.

[57] H. Li et al., "The melanocortin action is biased toward protection from weight loss in mice," *Nature Commun.*, vol. 14, no. 1, p. 2200, Apr. 2023.

[58] H. Zheng et al., "A potential role for hypothalamomedullary POMC projections in leptin-induced suppression of food intake," *Amer. J. Physiol.-Regulatory, Integrative Comparative Physiol.*, vol. 298, no. 3, pp. 720–728, Mar. 2010.

[59] Y. S. Mineur et al., "Nicotine decreases food intake through activation of POMC neurons," *Science*, vol. 332, no. 6035, pp. 1330–1332, Jun. 2011.

[60] J. Kubanek, P. Shukla, A. Das, S. A. Baccus, and M. B. Goodman, "Ultrasound elicits behavioral responses through mechanical effects on neurons and ion channels in a simple nervous system," *J. Neurosci.*, vol. 38, no. 12, pp. 3081–3091, Mar. 2018.

[61] W. J. Tyler, Y. Tufail, M. Finsterwald, M. L. Tauchmann, E. J. Olson, and C. Majestic, "Remote excitation of neuronal circuits using low-intensity, low-frequency ultrasound," *PLoS ONE*, vol. 3, no. 10, p. e3511, Oct. 2008.

[62] S. Yoo, D. R. Mittelstein, R. C. Hurt, J. Lacroix, and M. G. Shapiro, "Focused ultrasound excites cortical neurons via mechanosensitive calcium accumulation and ion channel amplification," *Nature Commun.*, vol. 13, no. 1, p. 493, Jan. 2022.

[63] S. Ibsen, A. Tong, C. Schutt, S. Esener, and S. H. Chalasani, "Sonogenetics is a non-invasive approach to activating neurons in caenorhabditis elegans," *Nature Commun.*, vol. 6, no. 1, p. 8264, Sep. 2015.

[64] B. Sorum, R. A. Rietmeijer, K. Gopakumar, H. Adesnik, and S. G. Brohawn, "Ultrasound activates mechanosensitive TRAAK $K^+$ channels through the lipid membrane," *Proc. Nat. Acad. Sci. USA*, vol. 118, no. 6, 2021, Art. no. e2006980118.

[65] M. Plaksin, E. Kimmel, and S. Shoham, "Cell-type-selective effects of intramembrane cavitation as a unifying theoretical framework for ultrasonic neuromodulation," *Eneuro*, vol. 3, no. 3, 2016. [Online]. Available: http://dx.doi.org/10.1523/ENEURO.0136-15.2016

[66] K. Yu, X. Niu, E. Krook-Magnuson, and B. He, "Intrinsic functional neuron-type selectivity of transcranial focused ultrasound neuromodulation," *Nature Commun.*, vol. 12, no. 1, p. 2519, May 2021.

[67] K. R. Murphy et al., "A tool for monitoring cell type–specific focused ultrasound neuromodulation and control of chronic epilepsy," *Proc. Nat. Acad. Sci. USA*, vol. 119, no. 46, Nov. 2022, Art. no. e2206828119.

[68] T. Sato, M. G. Shapiro, and D. Y. Tsao, "Ultrasonic neuromodulation causes widespread cortical activation via an indirect auditory mechanism," *Neuron*, vol. 98, no. 5, pp. 1031–1041, Jun. 2018.

[69] H. Guo et al., "Ultrasound produces extensive brain activation via a cochlear pathway," *Neuron*, vol. 98, no. 5, pp. 1020–1030, Jun. 2018.

[70] W. J. Tyler, S. W. Lani, and G. M. Hwang, "Ultrasonic modulation of neural circuit activity," *Current Opinion Neurobiol.*, vol. 50, pp. 222–231, Jun. 2018.

[71] J. Ye et al., "Ultrasonic control of neural activity through activation of the mechanosensitive channel MscL," *Nano Lett.*, vol. 18, no. 7, pp. 4148–4155, Jul. 2018.

[72] Q. Jiang et al., "Temporal neuromodulation of retinal ganglion cells by low-frequency focused ultrasound stimulation," *IEEE Trans. Neural Syst. Rehabil. Eng.*, vol. 26, no. 5, pp. 969–976, May 2018.

[73] W. Zhou et al., "Ultrasound neuro-modulation chip: Activation of sensory neurons in caenorhabditis elegans by surface acoustic waves," *Lab Chip*, vol. 17, no. 10, pp. 1725–1731, 2017.

[74] Y. Wang et al., "Ultrasound stimulation of periaqueductal gray induces defensive behaviors," *IEEE Trans. Ultrason., Ferroelectr., Freq. Control*, vol. 68, no. 1, pp. 38–45, Jan. 2021.

[75] M. Mohammadjavadi, P. P. Ye, A. Xia, J. Brown, G. Popelka, and K. B. Pauly, "Elimination of peripheral auditory pathway activation does not affect motor responses from ultrasound neuromodulation," *Brain Stimulation*, vol. 12, no. 4, pp. 901–910, Jul. 2019.

[76] W. Legon, P. Bansal, R. Tyshynsky, L. Ai, and J. K. Mueller, "Transcranial focused ultrasound neuromodulation of the human primary motor cortex," *Sci. Rep.*, vol. 8, no. 1, p. 10007, Jul. 2018.

[77] W. Lee et al., "Transcranial focused ultrasound stimulation of human primary visual cortex," *Sci. Rep.*, vol. 6, no. 1, p. 34026, Sep. 2016.

[78] W. Lee, H. Kim, Y. Jung, I.-U. Song, Y. A. Chung, and S.-S. Yoo, "Image-guided transcranial focused ultrasound stimulates human primary somatosensory cortex," *Sci. Rep.*, vol. 5, no. 1, p. 8743, Mar. 2015.

[79] B. C. Gibson et al., "Increased excitability induced in the primary motor cortex by transcranial ultrasound stimulation," vol. 9, p. 1007, Nov. 2018.

[80] W. Legon et al., "A retrospective qualitative report of symptoms and safety from transcranial focused ultrasound for neuromodulation in humans," *Sci. Rep.*, vol. 10, no. 1, p. 5573, Mar. 2020.